IEEE Photonics Journal
An IEEE Photonics Society Publication

Open Access

Single Exposure Optical Image Watermarking Using a cGAN Network

Volume 13, Number 2, April 2021

Jiaosheng Li
Yuhui Li
Ju Li
Qinnan Zhang
Guo Yang
Shimei Chen
Chen Wang
Jun Li

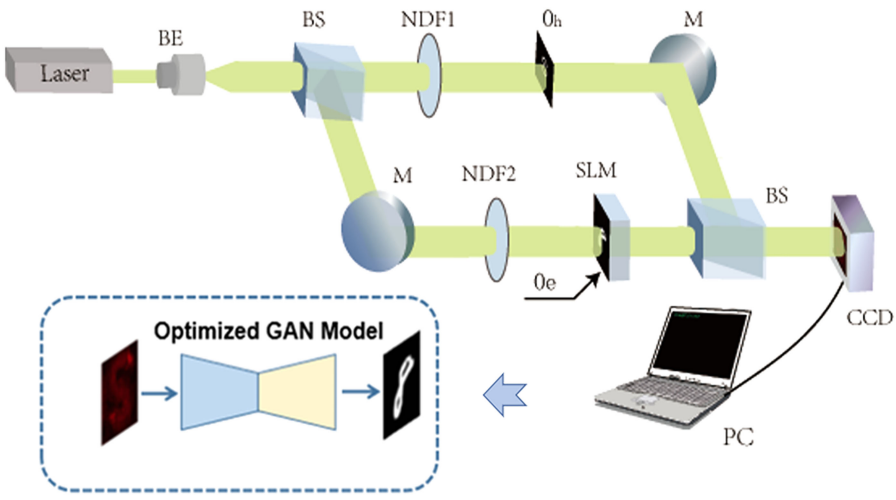

The schematic of the cGAN-based optical image watermarking method, which consists of two process: watermarking process and decryption process.

DOI: 10.1109/JPHOT.2021.3068299

Single Exposure Optical Image Watermarking Using a cGAN Network

Jiaosheng Li,[1,2] **Yuhui Li**,[1] **Ju Li**,[1] **Qinnan Zhang**,[3] **Guo Yang**,[1] **Shimei Chen**,[1] **Chen Wang**,[4] **and Jun Li**[1]

[1]Guangdong Provincial Key Laboratory of Quantum Engineering and Quantum Materials, South China Normal University, Guangzhou 510006, China
[2]School of Photoelectric Engineering, Guangdong Polytechnic Normal University, Guangzhou 510665, China
[3]School of Electrical Engineering and Intelligentization, Dongguan University of Technology, Dongguan 523808, China
[4]School of Electronic Science and Engineering, Nanjing University, Nanjing 210000, China

DOI:10.1109/JPHOT.2021.3068299

Manuscript received January 17, 2021; revised March 15, 2021; accepted March 19, 2021. Date of publication March 23, 2021; date of current version April 9, 2021. This work was supported in part by the National Natural Science Foundation of China under Grant 61805086 and in part by China Postdoctoral Science Foundation under Grant 2018M643114. (Jiaosheng Li, Yuhui Li, and Ju Li contributed equally to this work). Corresponding author: Jun Li (e-mail: lijunc@126.com).

Abstract: A single exposure optical image watermarking framework based on deep learning (DL) is proposed in this paper, and original watermark image information can be reconstructed from only single-frame watermarked hologram by using an end-to-end network with high-quality. First, the single exposure watermarked hologram is acquired with our presented phase-shifted interferometry based optical image watermarking (PSOIW) frame, and then all holograms and corresponding watermark images are constructed to the train datasets for the learning of an end-to-end conditional generative adversarial network (cGAN), finally retrieved the watermark image well with the trained cGAN network using only one hologram. This DL-based method greatly reduces the recording or transmitting data burden by 1/4 compared with our presented PSOIW technique, and may provide a new way for the real-time 3D image/video security applications. The feasibility and security of the proposed method are demonstrated by the optical experiment results.

Index Terms: Optical image watermarking, image reconstruction, digital holography, deep learning, generative adversarial network.

1. Introduction

Deep learning (DL) obtains the approximation of the optimal model of the system through large amount of prior information. In the real imaging or security system, we can use the prior information to obtain more accurate parameters of the model through the computer. Based on this, DL has shown its advantages in many applications, such as optical imaging [1]–[3], phase recovery and holographic image reconstruction [4]–[6], computational ghost imaging [7], Cryptanalysis [8]–[10], etc. [11]. Convolutional networks [12] shows its powerful function in optical image reconstruction [1], [3], [13], and can be used to reconstruct the object wavefront directly from a single-shot in-line digital hologram [5], [6].

Optical image security technology has become an important research direction in the field of information security because of its advantages of high efficiency, high security, difficult to crack

and easy to store [14]–[17]. Since the double random phase encoding (DRPE) technology was put forward [18], optical image security technology has developed rapidly by introducing additional degrees of freedom, such as wavelength, propagation distance [18], degree of polarization [19]. By embedding the original information into the host information without destroying the form of the original host information, optical image watermarking can achieve the purpose of solving copyright protection and thus enhance the security [20]–[23], thus reducing the possibility of being violated. On this basis, the classical methods in cryptography are used to enhance the security of the watermarked information. Among the optical image watermarking technologies, phase-shifted interferometry based optical image watermarking (PSOIW) technology [21], [24]–[27] can not only make use of the spatial bandwidth product of CCD to record the hologram information, but also make up the shortage of in-line and off-axis digital holography. However, it needs to get multiple phase-shifting holograms with specific phase shifts and the usage of various optical encryption keys to realize image reconstruction. The amount of data transmitted is large, the resolution of reconstructing the original image from the recorded hologram is limited, and multiple recording will affect the dynamic application, which have been the main constraint in the application of optical image security.

Based on this, a high- quality and single exposure optical image watermarking framework based on deep learning (DL) is proposed to implement real-time watermark embedding with high-resolution in this paper. By using the prior information between the watermarked image and the object image, the proposed method can obtain the approximation of watermarking model based on the optical inverse diffraction through the DL method. Based on the generative adversarial network (GAN) [28], by setting the corresponding constraints, that is, the watermarked image as the constraint of DL, the conditional generative adversarial network (cGAN) [29] can continuously learn the corresponding relationship between the watermarked image and the reconstructed image, so that only single- frame watermarked hologram is needed to realize the reconstruction of optical image watermarking. In the proposed method, the optical system no longer needs phase-shifting device, and the reconstruction process can be obtained without the parameters in optical inverse diffraction and the reconstruction result will not be affected by the system noise and other disturbances. Besides, only a hologram needs to be transmitted, so the transmission efficiency is greatly improved. In this paper, the feasibility and superiority of the method are verified by the experiment, including the image reconstruction results under different data volumes, generalization, security, and robustness are analyzed in detail.

2. Method Analysis

Here, a single exposure cGAN-based optical image watermarking framework is introduced. By using the prior data between the watermarked image and the object image, the watermarking model based on optical diffraction is obtained by cGAN, and the decryption process can be obtained without the parameters in optical inverse diffraction. The schematic of the proposed method is shown in Fig. 1, and the whole method consists of two process: watermarking process and decryption process. The watermarking process is implemented by PSOIW system, as shown in Fig. 1(a). A series of watermarked images are collected from the PSOIW system, and then the original image and the corresponding watermarked image are input to the PC end to train by the cGAN. After the training, the optimized generation network can be obtained to reconstruct the object image from watermarked hologram directly, as shown in Fig. 1(b).

2.1 Review of Optical Image Watermarking Based on Modified Mach-Zehnder Interferometer

The basic principle of optical image watermarking will briefly be introduced in this section. The schematic of optical image watermarking is showed in Fig. 1(a). The laser beam expanded by a beam expander (BE) is divided into an object beam and a reference beam by a beam splitter (BS). The object beam first irradiates the object image (Oe) loaded on the spatial light modulator

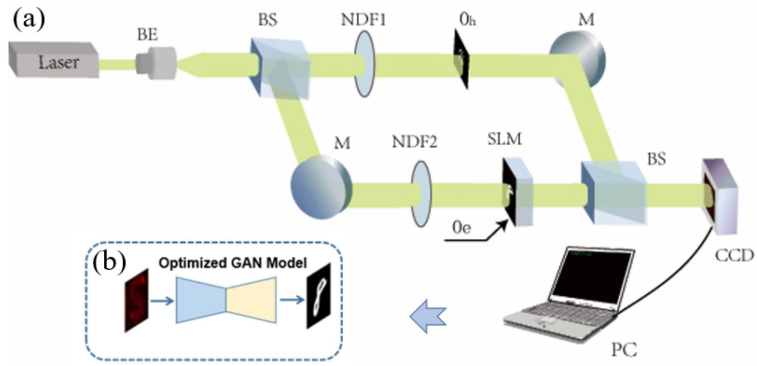

Fig. 1. The schematic of (a) the cGAN-based optical image watermarking method and (b) decryption process. BE, beam expander; BS, beam splitter; M, mirror; NDF, neutral density filters; SLM: spatial light modulator; Oe, object image; Oh, host image.

(SLM); the host image (O_h) is placed in the reference beam to achieve the modulation of the reference beam. The neutral density filters (NDF1 and NDF2) are used to adjust the light intensity ratio between the object beam and the modulated reference beam. Next, the object beam and the modulated reference beam will overlap to produce the hologram on the CCD, thus image watermarking is achieved.

Assuming that the transmissivity of the original image can be expressed as $O(x_0, y_0)$, then the complex amplitude of the original image on the CCD plane can be expressed as:

$$\psi_0(x, y) = Frt[O(x_0, y_0)] = A(x, y)\exp[i\phi(x, y)] \tag{1}$$

Where *Frt* represents the Fresnel transform of $O(x_0, y_0)$, then the complex amplitude distribution of the host image can be expressed as:

$$\psi_h(x, y) = A_h(x, y)\exp[i\phi_h(x, y)] \tag{2}$$

Therefore, the interference intensity distribution obtained on the CCD can be written as:

$$\begin{aligned} I(x, y) &= \left|\psi_0(x, y) + \psi_h(x, y)\right|^2 \\ &= A(x, y)^2 + A_h(x, y)^2 \\ &\quad + 2A(x, y)A_h(x, y)\cos[\phi_h(x, y) - \phi(x, y)] \end{aligned} \tag{3}$$

In the process of image watermarking, the original image is embedded in the diffraction field of the host image. Different watermarking effects can be achieved through adjusting the light intensity ratio of the object beam and the reference beam by adjusting two neutral density filters in the experimental system. Therefore, the hologram can look like the diffraction field of the host image when original image is embedded. The traditional reconstruction method needs to add a phase-shifting device in the experimental system to collect at least two-frame phase-shifting holograms of watermarked image and host image, and then use the multi-step phase-shifting method to reconstruct them. In the proposed method, the experimental data set can be built by continuously loading different original images on SLM, and a CCD is used to record the resulting interference fringes.

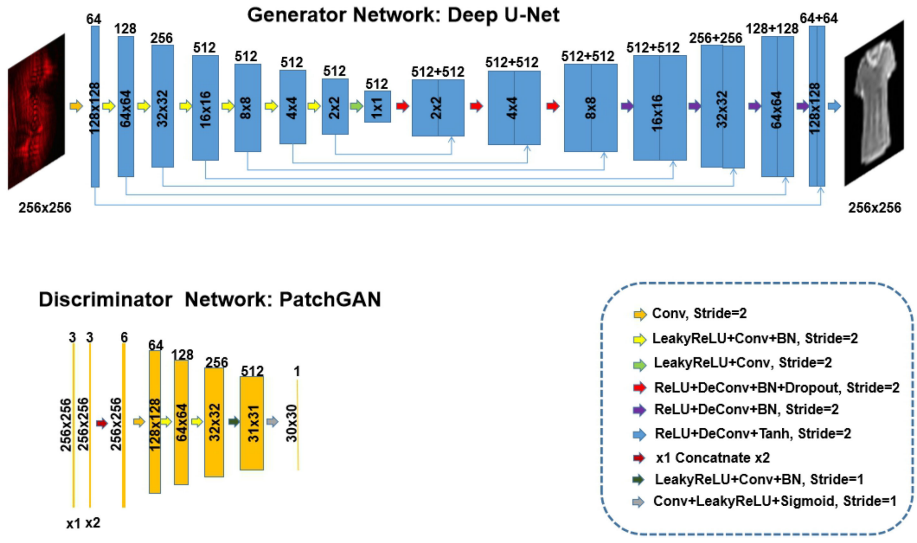

Fig. 2. The designed cGAN architecture, including generator network and discriminator network.

2.2 Learning-Based Decryption and Reconstruction From Single-Frame Watermarked Hologram

The proposed cGAN model in this paper can obtain the decryption and reconstruction results directly from single frame watermarked hologram, and the process is expressed as follows:

$$O' = \Psi_{\text{cGAN}}\{I\} \tag{4}$$

Where $\Psi_{\text{cGAN}}\{\cdot\}$ represents the mapping function between the watermarked hologram I and the label Oin the training process, and O'represents a preliminary estimate of the reconstructed image. This mapping can be optimized after training the cGAN model from N pairs of different label training data, and each pair has a known watermarked hologram I^n and label O^n, where $n = 1, 2, \ldots, N$. This training process is similar to the optimization process and can be expressed as

$$\hat{\Psi}_{\text{cGAN}} = \arg\min \frac{1}{N} \sum_{n=1}^{N} ||O^n - O'^n|| \tag{5}$$

$$\hat{O} = \hat{\Psi}_{\text{cGAN}}\{I\} \tag{6}$$

Where $\hat{\Psi}_{\text{cGAN}}\{\cdot\}$ represents the optimized cGAN model and $\hat{O}$ represents optimal estimation of reconstructed image by the optimized model, $||\cdot||$ is a loss function about the error between O^n and O'^n.

2.3 The Designed cGAN Architecture

In our scheme, a cGAN is developed to train the object images (training label) and the corresponding watermarked images (training data). The network structure diagram of cGAN is shown in Fig. 2, which consists of two parts, i.e., generator network and discriminating network. The watermarked image is firstly entered the generator network to get the estimated image of the corresponding object image, then the estimated image and the watermarked image will form a “fake image pair” and the watermarked image and the real object image form a “real image pair”. These two pairs of images are input into the discrimination network and the corresponding discrimination matrix are generated, respectively. Then the loss of the discriminators is calculated to optimize the parameters of the discrimination network. At the same time, the discriminator loss is also involved

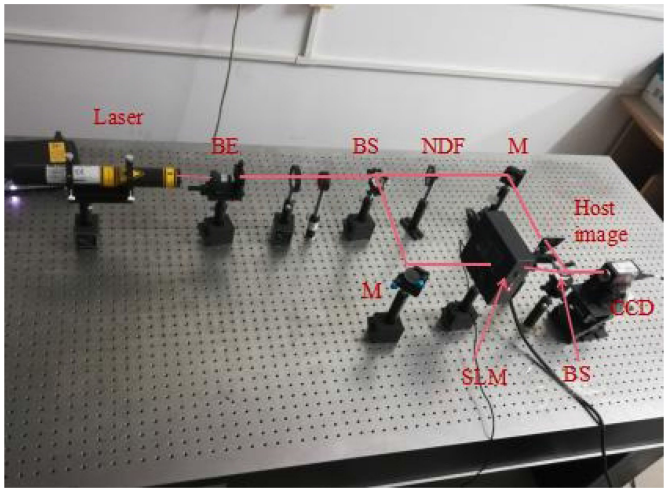

Fig. 3. The experimental setup of the cGAN-based optical image watermarking system. BE, beam expander; BS, beam splitter; M, mirror; NDF, neutral density filters; SLM: spatial light modulator.

in the optimization of the parameters of the generation network, so as to continuously optimize the network model. Finally, when the discrimination network cannot distinguish the generated image (that is, the generated image is very close to the label image), the DL model used for retrieving the object image from the watermarked hologram is learned by the generated network.

In the diagram of generator network, the input and output of generator network are set to be watermarked image and the object image. The watermarked image firstly passes through 8 downsampling convolution layers to get the feature maps of watermarked image, and then the estimate of the object image is produced by passing through 8 upsampling convolution layers. In addition, the downsampling layer and the upsampling layer of the generator can supplement the high-frequency information of the reconstructed object image through the skip connections. The discrimination network adopts PatchGAN structure [29], as shown in Fig. 2, and the input is "real image pair" or "fake image pair". The "image pair" is first concatenated by channels, and then a distinguish matrix with the size of 30 $\times$ 30 is obtained by five downsampling layers. In addition, the Dropout ($p = 0.5$) is introduced to the first three upsampling layers of the generator network to prevent over fitting. After training, the trained DL model can be used to retrieve the object image from the watermarked hologram, and the calculation time of retrieving single frame image is 0.07s. Here, the designed cGAN architecture is implemented by Python version 3.7 on a PC with Nvidia Geforce GTX1080Ti GPU.

3. Experimental Results and Discussions

3.1 Experimental System Analysis

The experimental setup is schematically showed in Fig. 3. A He-Ne laser (REO/30989) with the wavelength of 633 nm is used as illumination source. After the laser beam is expanded, the object beam and the reference beam modulated by the host image are respectively obtained through beam splitter (BS) to produce the watermarked hologram on CCD plane. Where SLM (FSLM07U-A) is used to load the object image, and a letter of 'S' is used as the host image. The images used as object image are handwritten-digit patterns from the MNIST database [30] and fashion-MNIST database (8-bit grayscale images with 28 $\times$ 28 pixels) [31], which are widely used for DL. The resulting hologram are recorded by a CCD (AVT Pike F-421B/C) with the size of 2048 $\times$ 2048 pixels, and the pixel pitch is 7.4 um. By loading a series of object images on SLM, the corresponding watermarked image can be collected by CCD. Instead of making great effort to retrieve the object

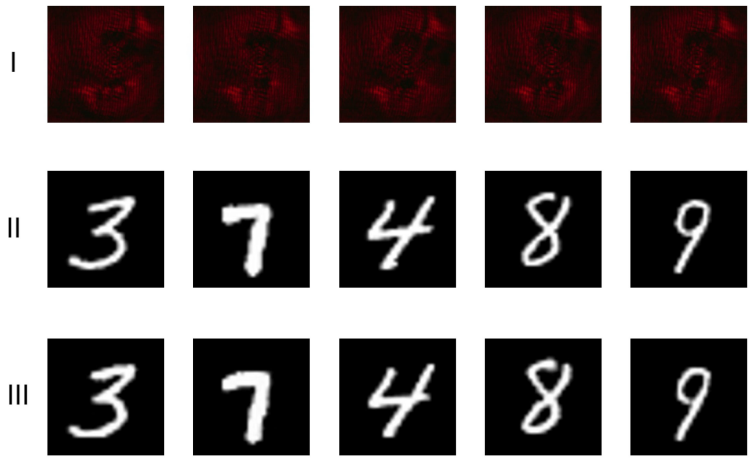

Fig. 4. Retrieved images of MNIST test data: (i) 5 testing watermarked images from 300 testing data, (ii) ground truth (original object images), (iii) the retrieved object images by trained cGAN based-watermarking method.

light wave by using multi-step phase-shifting method with various security keys, the object image can be retrieved directly by using a trained machine-learning model. 3000 images are loaded on the SLM to perform watermark and 2700 of the corresponding watermarked images are used as the training data and the rest 300 as the testing data. The central 256 $\times$ 256 pixels of them are chosen to perform the training.

3.2 Results and Discussions

First, a set of watermarked images embedded by handwritten-digit patterns from the MNIST database are used for training, the retrieved results are showed in Fig. 4. Where the first row is the watermarked holograms, the corresponding ground truth and the reconstructed images are showed in the second and third row, respectively. Structural similarity index (SSIM) is a quality metric used to measure the similarity between two images. Different from the traditional error summation method, SSIM is designed to model any image distortion as a combination of three factors that are correlation loss, luminance and contrast distortion. For quantitative analysis, SSIM is used and defined as:

$$SSIM\left(f, f_0\right) = \frac{\left(2\mu_f\mu_{f_0} + c_1\right)\left[2\mathrm{cov}(f, f_0) + c_1\right]}{\left(\mu_f^2 + \mu_{f_0}^2 + c_1\right) + \left(\sigma_f^2 + \sigma_{f_0}^2 + c_2\right)} \tag{7}$$

where f and f_0 denote the intensity distribution of reconstructed image and ground truth, respectively; μ_f and μ_{f_0} are the mean values of the image of f and f_0, and $\mathrm{cov}(f, f_0)$ represents the covariance between f and f_0, σ_f and σ_{f_0} are the standard deviations of f and f_0, respectively. c_1 and c_2 are the regularization parameters. By analysis, the averaged SSIM of the retrieved handwritten-digit patterns is 0.963. Evidently, only one hologram is needed without the usage of various optical encryption keys to retrieve the object images, and the retrieved images are of high quality compared with the ground truth. Moreover, the noise in the experimental system has almost no effect on the quality of the reconstructed image.

In order to further verify the feasibility of the method, 2700 fashion-MNIST database are used for training, in which the image content is more complex and the details are more abundant, and the retrieved results are distributed as shown in Fig. 5. The watermarked holograms, corresponding ground truth and the reconstructed images are showed in the first, second and third row of Fig. 5. The averaged SSIM of the retrieved fashion-MNIST patterns is 0.86. Moreover, it can be seen from the collar and the pattern of the clothes in the retrieved images, the retrieved images are of high

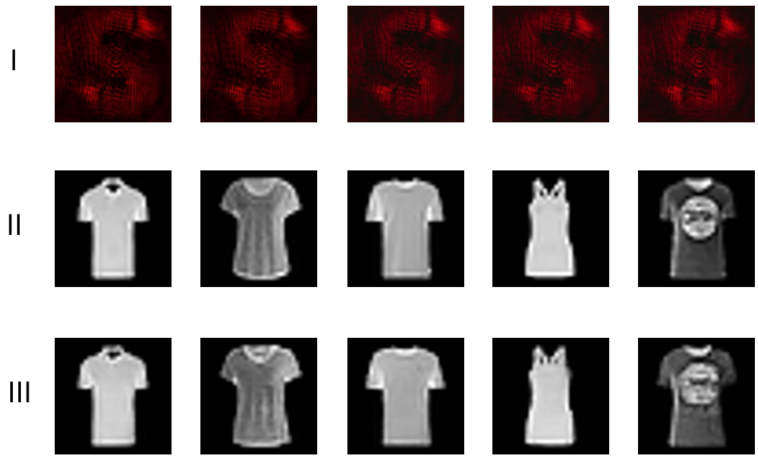

Fig. 5. Retrieved images of fashion-MNIST test data: (i) 5 testing watermarked images from 300 testing data, (ii) ground truth (original object images), (iii) the retrieved object images by trained cGAN based-watermarking method.

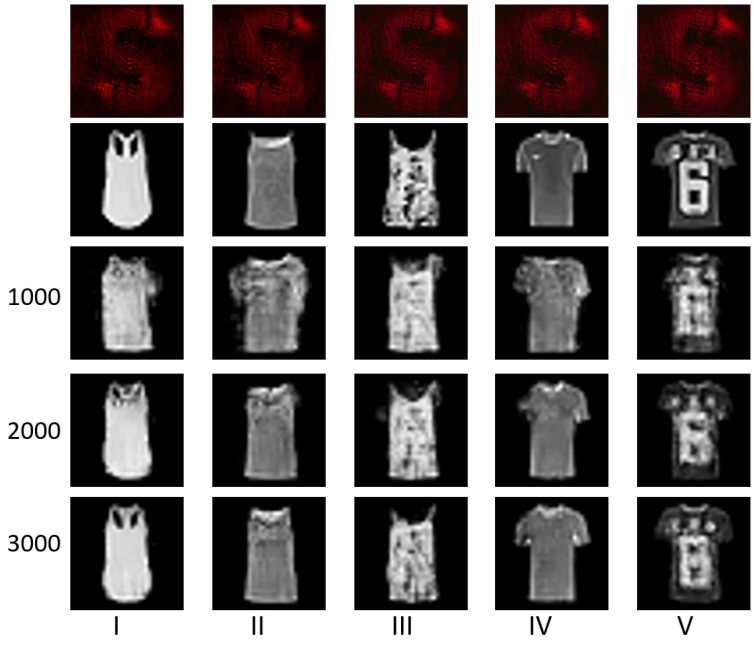

Fig. 6. Retrieved images under different data volumes.

quality, in which the retrieved information can be visualized and the high-frequency features are retained.

We also analyze the reconstructed results of fashion-MNIST test data with different data volumes. Under the same parameter setting, 1000, 2000 and 3000 experimental pictures are applied respectively, and then predicted by using the same test images. The reconstructed results are shown in Fig. 6. Where the watermarked images and the corresponding ground truth are showed in the first and second row, and the reconstructed images with different data volumes are showed in the last three rows, respectively. To quantify the performance of the reconstructed image under different data volumes during the training process, the correlation coefficient (CC) and normalized

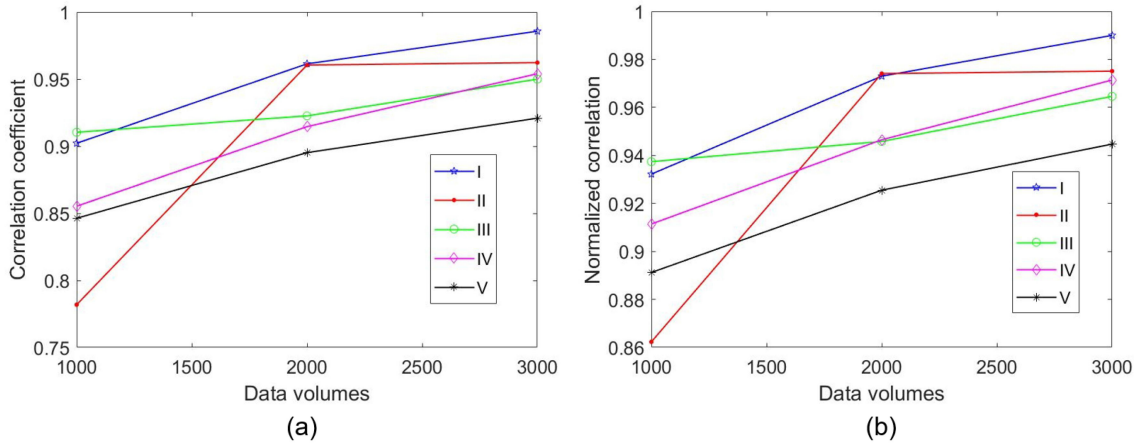

Fig. 7. Correlation coefficient and normalized correlation values under different data volumes.

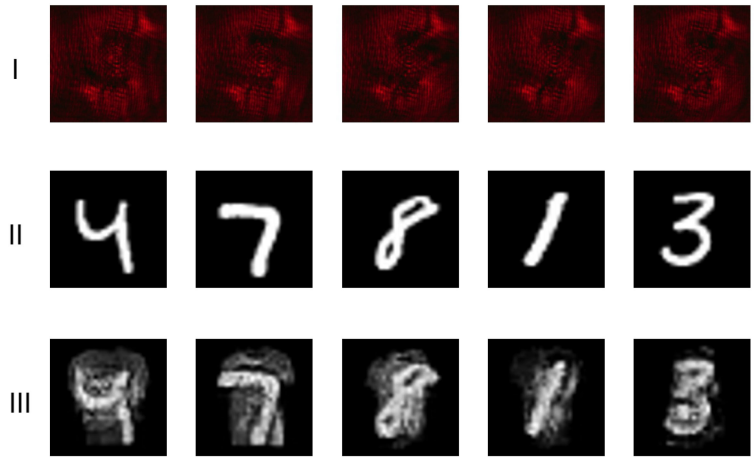

Fig. 8. Network generalization test results. (i) watermarked images embedded by MNIST handwritten data, (ii) ground truth (original object images), (iii) the object images retrieved form the network trained by fashion-MNIST test data.

correlation (NC) are introduced, in which the CC can be defined as:

$$C = \mathrm{cov}(f, f_0)(\sigma_f, \sigma_{f_0})^{-1} \tag{8}$$

The CC values and NC values between the reconstructed images and the ground truth under different data volumes are plotted in Figs. 7(a) and (b), in which the data volume changes from 1000 to 3000 with an interval of 1000. It can be seen from the results that with the increase of the number of data sets, the CC values, NC values and the quality of reconstructed image are improving accordingly. This shows that the quality of image restoration is directly related to the number of training data sets, but due to the limitations of experimental conditions and the time-consuming process of data set acquisition, we only collected 3000 experimental images for training, and the improvement of image quality in the later stage can be obtained through the increase of data volumes.

In addition, to examine the generalization of the trained neural network model, here, we use it to recover the object images that are different from those in the training set. For convenience, we test it with the MNIST handwritten data set and the reconstructed images are shown in Fig. 8. The

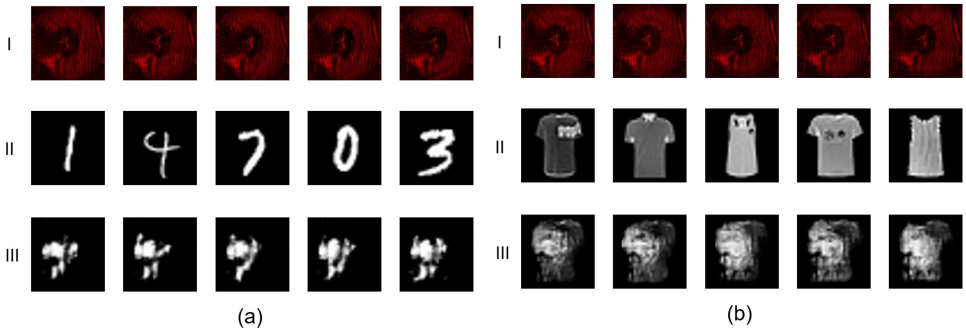

Fig. 9. Retrieved images with incorrect host information. (a) MNIST test data, (b) fashion-MNIST test data.

watermarked images embedded by the MNIST database is showed in the first row, and the second and third row are the corresponding ground truth and the reconstructed images, respectively. Although the network was trained by using the fashion-MNIST test data, it is clearly seen that it can be used to reconstruct the different object images from MNIST handwritten data set, which shows that cGAN network can obtain the mathematical model of image reconstruction by DL well, and different object images embedded in the optical image watermarking system can be reconstructed according to the optimized reconstruction network. However, due to the limited experimental data, the reconstructed image is a little fuzzy and the high-frequency details are lost, which can improve the performance by increasing the amount of data in the training set.

Following, the security of the optical image watermarking method is discussed in this section. Keeping the original image reconstruction network trained by cGAN with 2700 training data unchanged (the letter 'S' is used as the host image), the host image of the optical image watermarking system is changed to 'C', and the recorded watermarked image from MNIST test data and fashion-MNIST test data are input into the cGAN-based reconstruction network. The reconstruction results are shown in Fig. 9, in which the first row is the watermarked holograms, the corresponding ground truth and the reconstructed images with the wrong key are showed in the second and third row, respectively. The results indicate that when the host image information is missing, the correct object information cannot be obtained completely, which further proves the security of the optical image watermarking method. In addition, the results show that the premise of the high-quality image reconstruction method is to get the correct key, and only the host image information in the optical image watermarking system needs to be changed to resist the attack of DL-based system.

At last, the robustness of our method against rotation, shear, noise and JPEG compression attacks are investigated. Taking the MNIST test data as an example, the test experimental holograms are rotated anticlockwise by different degrees are input into the cGAN-based reconstruction network. The reconstruction results are shown in Fig. 10(a), in which the ground truth are given in the first row, and the reconstructed images with the rotation angle of 1, 2 and 4 degree are showed in the second, third and fourth row, respectively. Besides, another set of watermarked holograms with different shear ratio are input into the cGAN-based reconstruction network for deciphering and the Fig. 10(b) showed the reconstruction results. The first row shows the ground truth, and the reconstructed images with the shear ratio of 10%, 15% and 20% are present in the second, third and fourth row, respectively. Although the information is partially lost at the shear ratio of 20%, the correct handwritten numbers can still be obtained. Similarly, the white additive Gaussian noise of zero-mean with the standard deviation of 0.03, 0.05 and 0.07 are added to the holograms to test the robustness of the method, and the reconstruction results are shown in Fig. 11(a), where the ground truth are given in the first row. Finally, JPEG compression are implemented on the test holograms with the quality factor of 15, 25 and 35, and Fig. 11(b) showed the reconstruction results. These results obviously prove that the method is robust to the rotation, shear, noise and JPEG compression attacks.

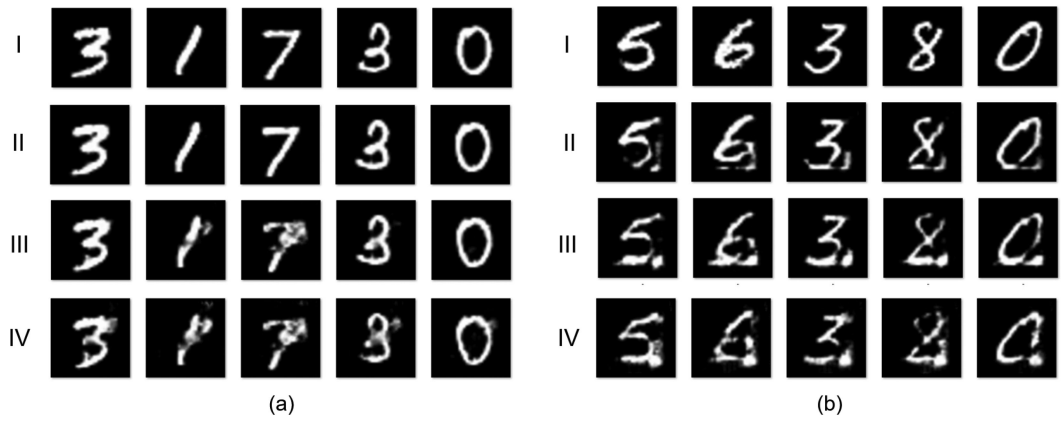

Fig. 10. The robustness of the proposed method against (a) rotation attack and (b) shear attack.

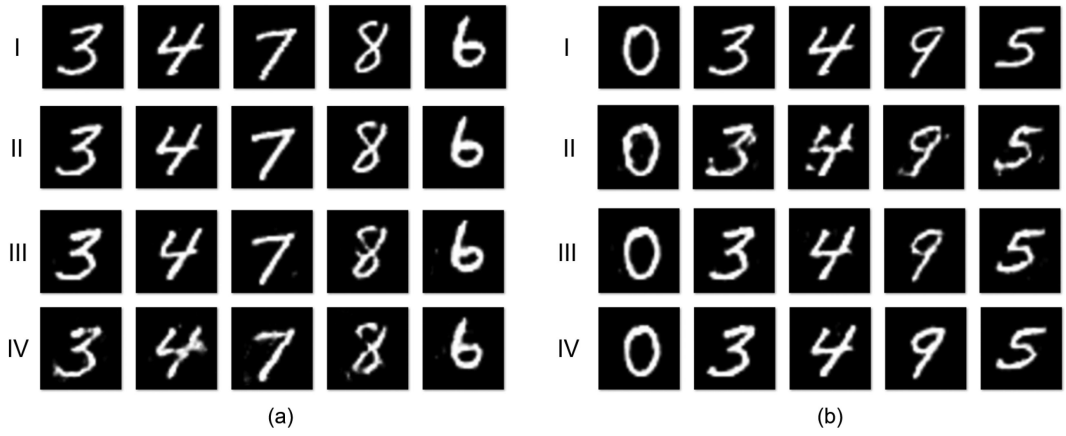

Fig. 11. The robustness of the proposed method against (a) noise attack and (b) JPEG compression attack.

4. Conclusion

In this paper, a single exposure optical image watermarking framework based on DL is proposed, in which an end-to-end cGAN is used to train the physical model of the watermarking system, and finally the physical model of the system is approached. In the proposed method, only a single hologram is needed to achieve high-quality decryption, the transmission efficiency is greatly improved. And the optical system does not need the phase-shifting device, the decryption results can be obtained without the parameters in optical inverse diffraction and will not be affected by the system noise and other disturbances, which is convenient for practical application. The feasibility and superiority of this method are verified by the experimental results, which reveals that the proposed method can provide a practical scheme to resist DL attacks and realize real-time and variable optical watermark embedding and extraction in the all-optical network, such as authenticity of identification, real-time video security transmission and naked-eye 3D Television, etc.

References

[1] A. Sinha, J. Lee, S. Li, and G. Barbastathis, "Lensless computational imaging through deep learning," *Optica*, vol. 4, no. 9, pp. 1117–1125, 2017.

[2] Y. Li, Y. Xue, and L. Tian, "Deep speckle correlation: A deep learning approach towards scalable imaging through scattering media," *Optica*, vol. 5, no. 10, pp. 1181–1190, 2018.
[3] S. Li, M. Deng, J. Lee, A. Sinha, and G. Barbastathis, "Imaging through glass diffusers using densely connected convolutional networks," *Optica*, vol. 5, no. 7, pp. 803–813, 2018.
[4] Y. Rivenson, Y. Zhang, H. Günaydın, D. Teng, and A. Ozcan, "Phase recovery and holographic image reconstruction using deep learning in neural networks," *Light-Sci. Appl.*, vol. 7, no. 2, 2017, Art. no. 17141.
[5] H. Wang, M. Lyu, and G. Situ, "eHoloNet: A learning-based end-to-end approach for in-line digital holographic reconstruction," *Opt. Exp.*, vol. 26, no. 18, pp. 22603–22614, 2018.
[6] K. Wang, K. Qian, J. Di, and J. Zhao, "Y4-Net: A deep learning solution to one-shot dual-wavelength digital holographic reconstruction," *Opt. Lett.*, vol. 45, no. 15, pp. 4220–4223, 2020.
[7] M. Lyu *et al.*, "Deep-learning-based ghost imaging," *Sci. Rep.*, vol. 7, no. 1, 2017, Art. no. 17865.
[8] L. Zhou, Y. Xiao, and W. Chen, "Machine-learning attacks on interference-based optical encryption: Experimental demonstration," *Opt. Exp.*, vol. 27, no. 18, pp. 26143–26154, 2019.
[9] H. Hai, S. Pan, M. Liao, D. Lu, W. He, and X. Peng, "Cryptanalysis of random-phase-encoding-based optical cryptosystem via deep learning," *Opt. Exp.*, vol. 27, no. 15, pp. 21204–21213, 2019.
[10] W. He, S. Pan, M. Liao, D. Lu, and X. Peng, "A learning-based method of attack on optical asymmetric cryptosystems," *Opt. Lasers Eng.*, vol. 138, 2021, Art. no. 106415.
[11] G. Barbastathis, A. Ozcan, and G. Situ, "On the use of deep learning for computational imaging," *Optica*, vol. 6, no. 8, pp. 921–943, 2019.
[12] O. Ronneberger, P. Fischer, and T. Brox, "U-Net: Convolutional networks for biomedical image segmentation," in *Proc. Int. Conf. Med. Image Comput. Comput.-Assist. Intervention*, 2015, pp. 234–241.
[13] T. Nguyen, V. Bui, V. Lam, C. Raub, L. Chang, and G. Nehmetallah, "Automatic phase aberration compensation for digital holographic microscopy based on deep learning background detection," *Opt. Exp.*, vol. 25, no. 13, pp. 15043–15057, 2017.
[14] J. Li, J. Li, L. Shen, Y. Pan, and R. Li, "Optical image encryption and hiding based on a modified Mach-Zehnder interferometer," *Opt. Exp.*, vol. 22, no. 4, pp. 4849–4860, 2014.
[15] W. Chen, B. Javidi, and X. Chen, "Advances in optical security systems," *Adv. Opt. Photon.*, vol. 6, no. 2, pp. 120–155, 2014.
[16] J. Li, J. Li, Y. Pang, and R. Li, "Compressive optical image encryption," *Sci. Rep.*, vol. 5, 2015, Art. no. 10374.
[17] Q. Wang, D. Xiong, A. Alfalou, and C. Brosseauc, "Optical image encryption method based on incoherent imaging and polarized light encoding," *Opt. Commun.*, vol. 415, pp. 56–63, 2018.
[18] P. Refregier and B. Javidi, "Optical image encryption based on input plane and fourier plane random encoding," *Opt. Lett.*, vol. 20, no. 7, pp. 767–769, 1995.
[19] G. Situ and J. Zhang, "Double random-phase encoding in the Fresnel domain," *Opt. Lett.*, vol. 29, no. 14, pp. 1584–1586, 2004.
[20] F. Petitcolas, R. J. Anderson, and M. G. Kuhn, "Information hiding – A survey," *Proc. IEEE*, vol. 87, no. 7, pp. 1062–1078, 1999.
[21] S. Kishk and B. Javidi, "Watermarking of three-dimensional objects by digital holography," *Opt. Lett.*, vol. 28, no. 3, pp. 167–169, 2003.
[22] S. Liu, B. M. Hennelly, and J. T. Sheridan, "Digital image watermarking spread-space spread-spectrum technique based on double random phase encoding," *Opt. Commun.*, vol. 300, pp. 162–177, 2013.
[23] S. Jiao, C. Zhou, Y. Shi, W. Zou, and X. Lia," Review on optical image hiding and watermarking techniques," *Opt. Laser Technol.*, vol. 109, pp. 370–380, 2019.
[24] L. Cai, M. He, Q. Liu, and X. Yang, "Digital image encryption and watermarking by phase-shifting interferometry," *Appl. Opt.*, vol. 43, no. 15, pp. 3078–3084, 2004.
[25] J. Li *et al.*, "A one-time pad encryption method combining full-phase image encryption and hiding," *J. Opt.*, vol. 19, no. 8, 2017, Art. no. 085701.
[26] J. Li, J. Li, Y. Pan, and R. Li, "Optical image hiding with a modified Mach-Zehnder interferometer," *Opt. Lasers Eng.*, vol. 55, pp. 258–261, 2014.
[27] J. Li, T. Zhong, X. Dai, Y. C. R. Li, and T. Z, "Compressive optical image watermarking using joint Fresnel transform correlator architecture," *Opt. Lasers Eng.*, vol. 89, pp. 29–33, 2017.
[28] I. J. Goodfellow, "Generative adversarial nets," in *Adv. Neural Inf. Process. Syst.*, pp. 2672–2680, 2014.
[29] P. Isola, J. Zhu, and T. Zhou, "Image-to-image translation with conditional adversarial networks," in *Proc. IEEE Conf. Comput. Vis. Pattern Recognit.*, 2017, pp. 1125–1134.
[30] L. Deng, "The MNIST database of handwritten digit images for machine learning research," *IEEE Signal Process. Mag.*, vol. 29, no. 6, pp. 141–142, Nov. 2012.
[31] H. Xiao, K. Rasul, and R. Vollgraf, "Fashion-MNIST: A novel image dataset for benchmarking machine learning algorithms," 2017, *arXiv:1708.07747*.